J. Physiol. (1983), **337**, *pp.* 1–17
With 8 text-figures
Printed in Great Britain

KINETIC PROPERTIES OF CALCIUM CHANNELS OF TWITCH MUSCLE FIBRES OF THE FROG

BY J. A. SÁNCHEZ* AND E. STEFANI†

From the Department of Physiology and Biophysics, Centro de Investigación del IPN, Apartado Postal 14-740, Mexico, D.F. 07000 Mexico

(*Received 6 April 1982*)

SUMMARY

1. Calcium currents (I_{Ca}) were recorded in frog skeletal muscle fibres using the three-micro-electrode voltage-clamp technique. The sartorius muscle was bathed in TEA methanesulphonate saline with 350 mM-sucrose. 5 mM-3,4-diaminopyridine was added to the saline to minimize K^+ currents.

2. The I–V relationship for peak Ca^{2+} currents showed that I_{Ca} was detected at -40 mV and reached a maximum value at *ca.* -10 mV. No net inward current was recorded at potentials positive to *ca.* $+40$ mV.

3. Remaining K^+ currents (I_K) were recorded by replacing 10 mM-Ca^{2+} with 5·5 mM-Co^{2+}. They were not noticeably time-dependent up to $+20$ mV and would tend to diminish the amplitude of I_{Ca} without greatly affecting its time course.

4. I_{Ca} tail currents could be separated from non-linear capacity currents. Tail currents were measured 5 msec after repolarization and extrapolated to the end of the pulse.

5. I_{Ca} tail-current amplitudes at E_K were measured with pulses of different durations. The envelope of tail-current amplitudes declined with a time course similar or identical to that of inward current during a maintained depolarization. Consequently, the decline of inward current cannot be explained by an increase of outward I_K with time.

6. I_{Ca} inactivated with 9 sec prepulses which did not elicit detectable I_{Ca}. The fitted h_∞ curve had a mid point of $-33{\cdot}0$ mV and a steepness of 6·3 mV.

7. I_{Ca} between -30 mV and $+20$ mV could be described adequately using the Hodgkin–Huxley m^3h relationship. The fitted m_∞ curve had a mid point of $-35{\cdot}2$ mV and a steepness of 9·9 mV. The limiting Ca^{2+} permeability $\bar{P}_{Ca}$ was $1{\cdot}4 \pm 0{\cdot}4 \times 10^{-4}$ cm/sec.

INTRODUCTION

A slow Ca^{2+} action potential can be elicited in twitch muscle fibres of the frog by blocking K^+ channels with tetraethylammonium (TEA) and by removing the Cl^- shunt using an impermeant anion as SO_4^{2-} (Beaty & Stefani, 1976*a*). The Ca^{2+} current

* Present address: Department of Physiology and Biophysics, University of Washington, SJ-40, Seattle, WA 98195, U.S.A.

† To whom requests for reprints should be addressed.

(I_{Ca}) was later described using a voltage-clamp technique (Beaty & Stefani, 1976*b*; Stanfield 1977; Sánchez & Stefani, 1978).

The present study extends previous observations on the Ca^{2+} current, under conditions in which K^+ channels are more completely blocked, and focuses on some kinetic properties of the Ca^{2+} channels. The gating of the channels can be described

TABLE 1. Solutions (mM)

	Na^+	K^+	Ca^{2+}	TEA^+	Cl^-	$CH_3SO_3^-$
Normal saline	115	2·5	1·8	—	121·1	—
Na methanesulphonate saline	115	2·5	1·8	—	—	121·1
TEA methanesulphonate saline	—	2·5	10	115	—	137·5

The solutions also contained 1 mM-Tris maleate or 2 mM-imidazole buffers (pH 7·4). Tetrodotoxin (Calibiochem) ($\sim 10^{-6}$ M) and D-600 (10^{-5} M; methoxy derivative of iproveratril, Knoll Pharmaceuticals) were added from concentrated aqueous (10^{-4} g/ml.) and ethanol (10^{-3} g/ml.) solutions respectively. 3,4-DAP (5 mM) was dissolved directly in the saline. Mechanical artifacts were avoided by adding 350 mM-sucrose to the saline.

in principle in the Hodgkin and Huxley framework with independent gates for activation and inactivation.

Preliminary results have been presented to the Biophysical Society (Sánchez & Stefani, 1980) and to the 28th International Congress of Physiological Sciences (Stefani, Sánchez & Nicola Siri, 1981).

METHODS

Experiments were performed on sartorious muscles of cold-adapted (4–6 °C) *Rana temporaria* frogs. Muscles were dissected in normal saline (see Table 1), and then mounted stretched to about 30% of their slack length in an acrylic chamber. The normal saline was replaced by Na methanesulphonate saline and, after a wait of 10–15 min to permit equilibration of ionic gradients, the solution was replaced by TEA methanesulphonate saline. Finally, cooled (5 °C) hypertonic TEA methanesulphonate with 350 mM-sucrose to prevent mechanical artifacts was replaced in the bath. Thereafter experiments were performed at room temperature (22–26 °C).

Recording technique

Muscle fibres were voltage-clamped with the three-micro-electrode technique developed by Adrian, Chandler & Hodgkin, (1970) and described in detail elsewhere (Sánchez & Stefani, 1978; Nicola Siri, Sánchez & Stefani, 1980). Briefly, two micro-electrodes were positioned at distances l and $2l$ from the fibre end and were used to record the membrane potentials V_1 and V_2 respectively. V_1 or V_2 was controlled by a feed-back amplifier which injected current intracellularly at the distance $2l+l'$ from the fibre end. In initial experiments, stray capacity of micro-electrodes was carefully compensated, while in later experiments voltage followers with only 0·8 pF of input capacity were used so that capacity compensation was unnecessary.

Membrane current per unit of external surface (I_m, $\mu A/cm^2$) was calculated according to the equation (Adrian *et al.* 1970):

$$I_m = \frac{a(V_2 - V_1)}{3l^2 R_i}, \quad (1)$$

where a is the fibre radius and R_i is the resistivity of the myoplasm. l varied from 125 to 400 μm, l' from 20 to 50 μm and $R_i = 250\ \Omega$ cm in hypertonic solutions (Adrian *et al.* 1970). The radius

and the capacitance per unit external surface (C_m, $\mu F/cm^2$) were also calculated following the equations by Adrian *et al.* (1970). The holding potential was −90 mV.

The voltage and current signals were amplified and sampled digitally by a microcomputer (Sol 20, Processor Technology) at intervals ranging from 0·1 to 2 msec and stored on diskettes for further analysis. Digital conversion was accomplished by an eight-bit analog-to-digital converter interface (7 A+D, Cromemco).

Protocol and analysis

The experiments were designed to analyse the gating of Ca^{2+} channels. To this end, Na^+ channels were blocked by tetrodotoxin (TTX) and K^+ currents were largely suppressed by TEA and 3,4-diaminopyridine (3,4-DAP). Cl^- currents were virtually absent since Cl^- was replaced by the impermeant anion $CH_3SO_3^-$. Linear capacity and leakage currents were removed by scaling up and subtracting currents produced by small depolarizing steps (+10, +20 mV). The remaining currents are taken to be mainly Ca^{2+} currents.

Ca^{2+} currents were elicited by 1·8 sec depolarizations and were fitted to the function:

$$I_{Ca} = A\,(1-\exp(-t/\tau_m))^a\,(h_\infty-(h_\infty-1)\exp(-t/\tau_h)), \quad (2)$$

where A is an amplitude factor, τ_m, τ_h and h_∞ refer to the usual terminology introduced by Hodgkin & Huxley (1952) to describe sodium permeability of squid axons, and a is an integer constant.

We have assumed that at the holding potential (−90 mV) $h_0 = 1$ and $m_0 = 0$ which is very nearly true (see Results).

Fitting programs for the development of the kinetic model were written in Fortran IV, using the Patternsearch routine (Colquhoun, 1971) which minimizes the sum of the squared differences between the observations and the proposed function. To fit equation (2) to I_{Ca} a Univac 1100 computer was used. The program selected the best values of τ_m, τ_h and A; h_∞ was obtained from the steady-state inactivation curve, and a was not fitted, rather it contributed to the program as an integer constant with values between 1 and 4. Once the best values of a was selected, the rate constants of activation and inactivation could be calculated and fitted to the Hodgkin–Huxley equations. They were used subsequently to describe the voltage dependences of τ_m and τ_h.

Standard double-pulse techniques were used to follow the onset of inactivation at various potentials and to determine the steady-state inactivation curve. Similar procedures provided values of tail currents at different times and membrane potentials as described in the Results section.

Values are given as means ± S.E. of means with the number of observations in parentheses.

RESULTS

Calcium current

Fig. 1 shows digitized experimental records of I_{Ca} during steps from a holding potential of −90 mV. The recording solution was hypertonic TEA methanesulphonate with 5 mM-3, 4-DAP added. Each trace is the membrane current recorded as $V_2 - V_1$ samples at 2 msec per point during 1·8 sec depolarizing steps to different potentials (E (mV); see numbers at the right-hand side). Record *1* is the membrane current elicited by a control step (20 mV). In the following records the linear capacitive and ionic currents were subtracted as described in the Methods. In record *1* the capacity current and a small leakage current during the +20 mV control step can be seen. In this fibre the specific membrane conductance (G_m) was 0·04 mS/cm². The mean value of G_m in different fibres in TEA methanesulphonate saline was 0·08 ± 0·01 (12) mS/cm².

Records *2* and *3* show a transient outward current during the beginning of the pulse followed by a transient inward current on repolarization. These currents are similar to the charge movement described by Schneider & Chandler (1973) and Chandler, Rakowsky & Schneider (1976). Following Chandler *et al.* (1976), the amount of charge,

i.e. the time integral of the current, can be normalized for total fibre capacitance. The amount of charge during the 'on' period was 19·6 nC/μF and 23·5 nC/μF for steps to -25 and -20 mV respectively. Similar values were reported by Chandler *et al.* (1976). For large pulses, the 'on' charge was contaminated with remaining K^+ currents (compare records *4* and *8*), and Ca^{2+} tail currents contaminated the 'off' charge.

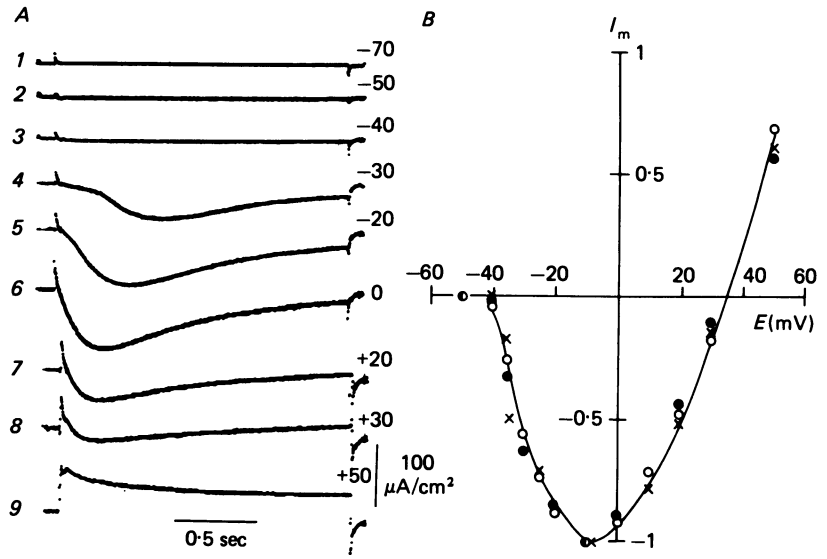

Fig. 1. *A*: membrane currents in TEA methanesulphonate with 5 mM-3,4-DAP and 350 mM-sucrose. Holding potential -90 mV. Numbers at right-hand side correspond to the membrane potential during 1·8 sec pulses. Record *1*: membrane currents during an initial step of $+20$ mV. Records *2–9* were subtracted for linear components. *B*: *I–V* relationship for peak currents for three different fibres (normalized values) in the same saline.

In record *2* no inward current could be detected during the pulse. In *3* there was a small inward Ca^{2+} current; this became evident in *4*, where the slowly developing Ca^{2+} current was followed abruptly by a much faster one. This could be due to the localization of Ca^{2+} channels in the tubular system (Nicola Siri *et al.* 1980; Almers, Fink & Palade, 1981), preventing an adequate voltage clamp. I_{Ca} increased in amplitude and became faster and steeper as the command-pulse amplitude was increased, being maximal at -10 mV. The maximum peak I_{Ca} after leak subtraction ranged from -40 to $-160\,\mu A/cm^2$ ($(80\pm10)\,\mu A/cm^2$ ($n = 14$)), in fibres with 30–60 μm radius.

With larger depolarizations I_{Ca} decreased in amplitude, approaching an apparent reversal potential of *ca.* $+40$ mV (records *8* and *9*). The *I–V* relationship for peak currents is shown in Fig. 1*B* for three different fibres (normalized values).

These inward currents were not maintained during the pulse, but decayed spontaneously after reaching a maximum. This suggests that I_{Ca} inactivates. However the participation during I_{Ca} of outward K^+ current and/or tubular Ca^{2+} depletion (Almers *et al.* 1981) is possible and will be analysed below. With large steps

there was a large initial outward current with a faster time course which spontaneously decayed. This current can be attributed to unblocked K^+ outward currents (Stanfield, 1970).

In summary, inward Ca^{2+} currents and remaining K^+ currents were recorded during prolonged depolarizations.

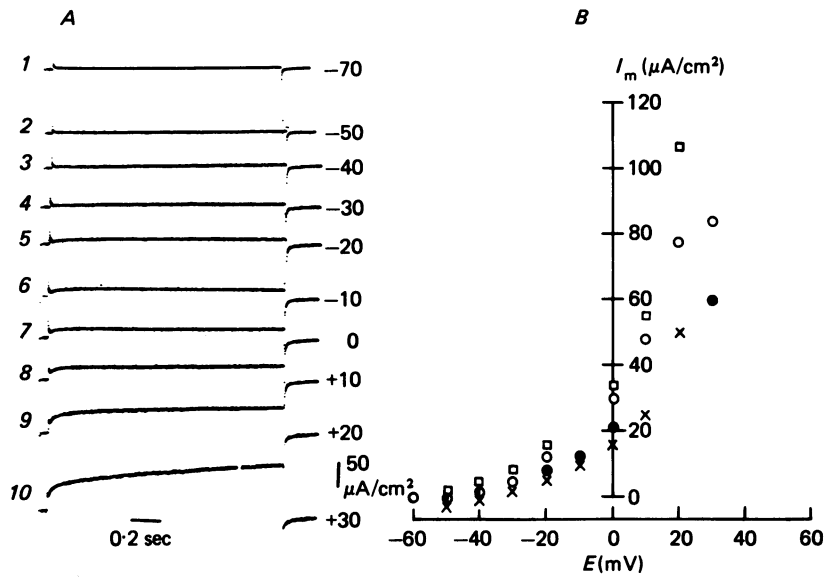

Fig. 2. *A*: membrane currents in TEA methanesulphonate saline with 5 mM-DAP and 350 mM-sucrose. External Ca^{2+} was replaced by 5·5 mM-Ca^{2+}. Holding potential −90 mV. Numbers at the right-hand side correspond to the membrane potential during 1·8 sec pulses. Record *1*: membrane currents during +20 mV pulse. Records *2–10* were subtracted for linear components. *B*: *I–V* relationship for maximum outward currents for four different fibres in the same saline.

Remaining K^+ currents

Since a quantitative analysis of gating of Ca^{2+} channels requires correction for any other ionic currents present, it was important to analyse the unblocked outward K^+ currents. To this end, experiments were performed in TEA methanesulphonate saline with Ca^{2+} replaced by Co^{2+}. To have an adequate replacement without major changes in the surface potential we previously measured the effective threshold of Na^+ currents.

In Na methanesulphonate saline with 10 mM-Ca^{2+} the threshold was $-42{\cdot}4 \pm 0{\cdot}7$ mV ($n = 7$). In the absence of Ca^{2+}, the threshold was $-44{\cdot}6 \pm 0{\cdot}7$ mV ($n = 8$) in 5 mM-Co^{2+} and $-40{\cdot}8 \pm 0{\cdot}7$ in 6 mM-Co^{2+} ($n = 6$). Thus, by interpolating these values, 10 mM-Ca^{2+} is adequately replaced by 5·5 mM-Co^{2+} for the Na^+ channel. This might not be the case for the Ca^{2+} channel but the difference is probably very small compared to the voltage range in which K^+currents were measured.

Fig. 2*A* shows records of membrane currents during depolarization steps from the holding potential of −90 mV. The muscle was bathed in TEA methanesulphonate saline in the absence of Ca^{2+} and with 5·5 mM-Co^{2+} and 5 mM-3,4-DAP. Having

replaced all Ca^{2+} by Co^{2+}, a blocker of the Ca^{2+} channel, no currents would be expected to flow through this channel, thus allowing the analysis of K^+ currents in isolation.

Record *1* corresponds to capacity and leakage currents during a +20 mV control step. Records *2–10* were corrected for linear components. The presence of a small outward current can be seen. This current was not noticeably time-dependent up to depolarizations of +10 mV (record *8*), and probably corresponds to non-linear leakage current. In six fibres tested, this outward current showed no time dependence for depolarizations up to 0 mV. For larger depolarizations a slowly developing outward current became evident which showed significant time dependence beyond +20 mV. Fig. 2*B* shows the *I–V* curve for different fibres in the same saline. In conclusion, remaining K^+ currents were mainly stationary for small depolarizations and would tend to diminish the amplitude of I_{Ca} but would not greatly affect its time course. However in this experiment we cannot rule out Ca^{2+}-activated K^+ currents (Fink &Lüttgau, 1976; Pallota, Magleby & Barrett, 1981).

Non-linear capacity currents and tail currents

The contribution of K^+ currents to I_{Ca} could be investigated further by tail-current experiments, but before an accurate measure of ionic currents during the 'tail' could be obtained it was important to determine the contribution of non-linear capacity currents.

Fig. 3 shows membrane currents in the same fibre during pulses of different durations; *A* shows non-linear capacity currents after subtraction of linear components during a 10 msec pulse to −10 mV. I_{Ca} was not detected with 10 msec pulse duration. The 'on' and 'off' currents decayed with a similar time course. The 'on' and 'off' charge displacements had similar values of 28·1 nC/μF and 30·8 nC/μF. Fig. 3*B* shows in the same fibre I_{Ca} elicited with a pulse which had the same amplitude but lasted 250 msec; the current recorded when the pulse was terminated is shown in *C*. The decay of I_{Ca} follows a single exponential (curve *b* in Fig. 3*D*) and the I_{Ca} at $t = 0$ could be accurately extrapolated. The points in curve *a* are the non-linear capacity current at the end of the 10 msec pulse shown in record *A*. It is clear that 5 msec after the termination of the pulse, the contribution of non-linear capacity currents is minimal. Thus, in order to measure instantaneous ionic currents, we extrapolated to time zero tail currents measured 5–10 msec after the end of the pulse.

Decay of Ca^{2+} current and K^+ activation

The set of experiments described above indicate that remaining K^+ currents play a minor role in the time course of I_{Ca} for membrane potentials below *ca.* +20 mV. It is then unlikely that the decline of I_{Ca} during maintained depolarizations can be explained on the basis of remaining K^+ activation. This view is confirmed in the experiment of Fig. 4*A* which shows the Ca^{2+} current decay in the same fibre during a 1·8 sec pulse to −10 mV from a holding potential of −90 mV. The semilogarithmic plot of I_{Ca} decay *vs.* time in Fig. 4*B* (●) indicates that I_{Ca} decayed almost exponentially with a time constant of 550 msec. The involvement of K^+ currents in this decay could be ruled out by measuring tail currents at different times at the holding potential (−90 mV) which is very close to E_K. One would not expect any significant contribution of K^+ currents to tail currents at this potential.

Record *A* in Fig. 4 shows tail currents at various times. The linear capacity and ionic components were subtracted from the total current to obtain the tail currents. The logarithm of the amplitudes of extrapolated tail currents at different pulse durations are plotted in Fig. 2*B* (○).

The graph shows that both I_{Ca} and tail-current envelopes followed similar exponential time courses, which indicates that the decay of I_{Ca} cannot be attributed to an outward K^+ current.

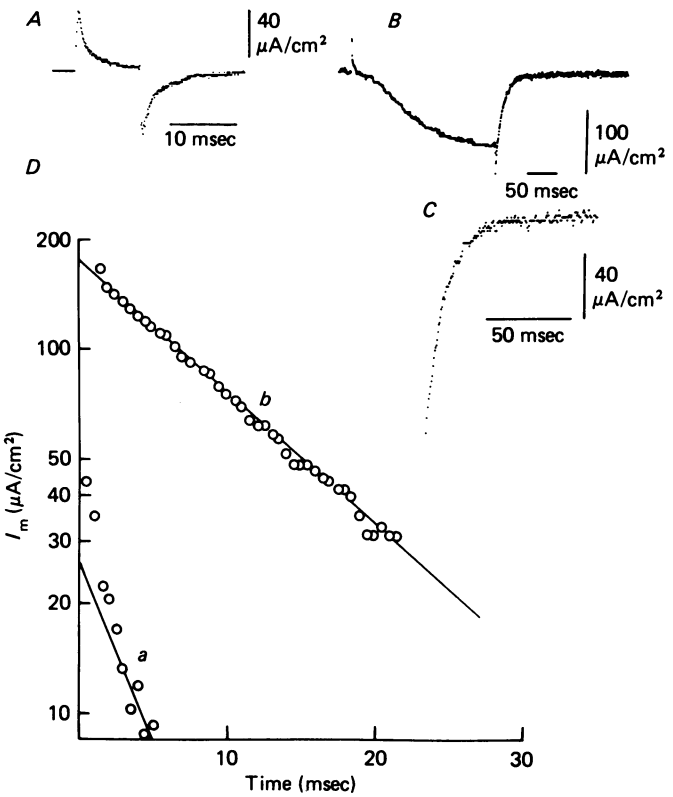

Fig. 3. Non-linear capacity current and Ca^{2+} tail currents. Same saline as in Fig. 1. Records were subtracted for linear components. Holding potential −90 mV and pulse to −10 mV. *A*: non-linear capacity currents during a 10 msec pulse, *B*: the same fibre with a longer pulse of 250 msec. *C*: tail current after the pulse was terminated at larger gain. The graph *D* is a semilogarithmic plot of the tail-current decay (curve *b*) (*C*) and of the non-linear capacity current at the end after 10 msec pulse (curve *a*) (*A*). The time constants of decay are 4·3 msec in *a* and 9·2 msec in *b*.

Decay of Ca^{2+} current and Ca^{2+} depletion in the tubular system

The Ca^{2+} channels are mainly located in the tubular system (Nicola Siri *et al.* 1980). Thus Ca^{2+} depletion could be another factor contributing to the decay of Ca^{2+} current as it was demonstrated in the cut fibre preparation (Almers *et al.* 1981). The depletion hypothesis was tested by measuring the time constant of I_{Ca} decay with different degrees of blockage with methoxyverapamil (D-600). If the decay of I_{Ca} is

related to intratubular Ca^{2+} depletion, one may expect that by reducing the size of I_{Ca} the intratubular Ca^{2+} depletion would be less important and the decay of I_{Ca} would slow down.

D-600 (10^{-5} M) has little effect when it is applied during a rest interval. Its ability to block I_{Ca} depends on the frequency of stimulation (McDonald, Pelzer & Trautwein,

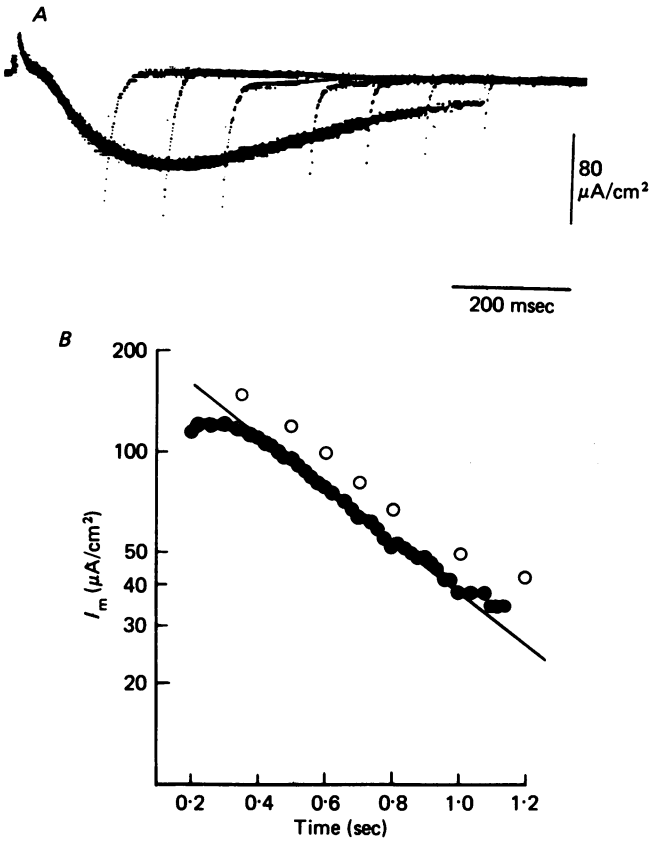

Fig. 4. *A*: tail-current amplitude measured for pulses to −10 mV with different durations. Same saline as in Fig. 1. Holding potential −90 mV. Records subtracted for linear components. Note the concomitant decay of I_{Ca} and tail-current amplitudes. *B*, semilogarithmic plot of I_{Ca} decay (filled circles) and of tail-current amplitudes for different pulse durations (open circles). Tail current maximum amplitudes were obtained by extrapolating to time zero tail currents measured 5 msec after the end of the pulse. The 'off' current points are larger than tail currents because of the 'off' charge movement.

1980) Record *1* in Fig. 5*A* shows I_{Ca} in TEA methanesulphonate with 5 mM-3,4-DAP in the presence of 10^{-5} M-D-600 after a period of rest of 7 min; records *2* and *3* show, in the same fibre, the Ca^{2+} current elicited by the fourth pulse at 1 stimulus per min and 2 stimuli per min respectively.

The time constant of I_{Ca} decay was 1060 msec in *1*, 1080 msec in *2* and 1180 msec in *3*. The graph shows in two different fibres the relationship between the rate of decay of I_{Ca} and the size of the peak current. I_{Ca} is referred to unit fibre volume since, under

the depletion hypothesis, the volume of the tubular system determines the rate of decay of I_{Ca} (Almers *et al.* 1981). It is apparent from the graph that between 10 mA/cm³ and 40 mA/cm³ there is almost no relation between the rate of decay and the current size. It is only for large currents that the rate of decay tends to increase, perhaps as a result of tubular depletion. However, it is necessary to consider possible

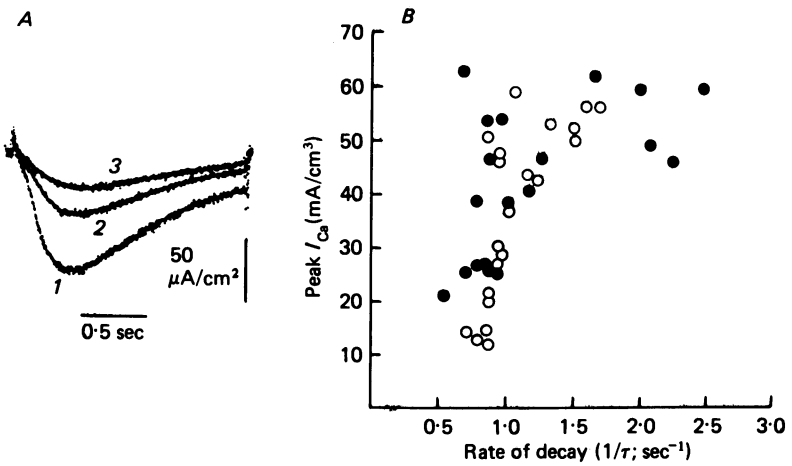

Fig. 5. Relationship between I_{Ca} decay and I_{Ca} amplitude at −10 mV. Same saline as in Fig. 1 with 10^{-5} M-D-600 added. Holding potential −90 mV. Records subtracted for linear components. In *A*, record *1* is the control I_{Ca}; records *2* and *3* show in the same fibre the fourth pulse at 1 stimulus and 2 stimulus per min respectively. The graph *B* shows the relationship between I_{Ca} peak amplitude and the rate of decay in two different fibres.

changes in the gating mechanism of the Ca^{2+} channels by D-600 since the peak time and the rate of onset of I_{Ca} are slowed down by D-600. For example, in the experiments shown in Fig. 5 the time constant of activation (τ_m) (see below) was 96 msec in *1*, 170 msec in *2* and 190 msec in *3*.

In conclusion, even though for large Ca^{2+} currents depletion may participate in its decay, the decline of the Ca^{2+} current during maintained depolarizations requires another explanation.

Inactivation of Ca^{2+} channels

The possibility that Ca^{2+} channels have a voltage-dependent inactivation was examined with double-pulse experiments. Fibres were selected with Ca^{2+} currents not larger than 40 mA/cm³ so that depletion if present was minimal.

Sequences of prepulses of different durations to several potentials were applied to determine the onset of inactivation. Peak I_{Ca} declined during a test pulse to 0 mV as the duration of the prepulse was increased. This decline followed a single exponential time course, and prepulses as long as 9 sec were necessary to reach the steady state for small depolarizations. The time constants (τ_h) for two such experiments are included in Fig. 8*B* (prepulses to −40 and to −46 mV with τ_h of 3 and 4·1 sec respectively).

Steady-state inactivation of peak I_{Ca} (h_∞) during a 0 mV test pulse was then

investigated with 9 sec prepulses to different potentials. In Fig. 6*A*, *1* shows the control I_{Ca} during the test pulse; in *2* a prepulse to −50 mV produced a slight decrease of I_{Ca} during the test pulse; this reduction became more evident as the amplitude of the prepulse was increased (records *3* and *4*).

Fig 6*B* shows that I_{Ca} was reduced during the test pulse to *ca.* 70 % of its control value by a prepulse to −50 mV (records *1* and *2*). In this case, a small Ca^{2+} current ($\sim 5\mu A/cm^2$) during the prepulse would have remained undetected.

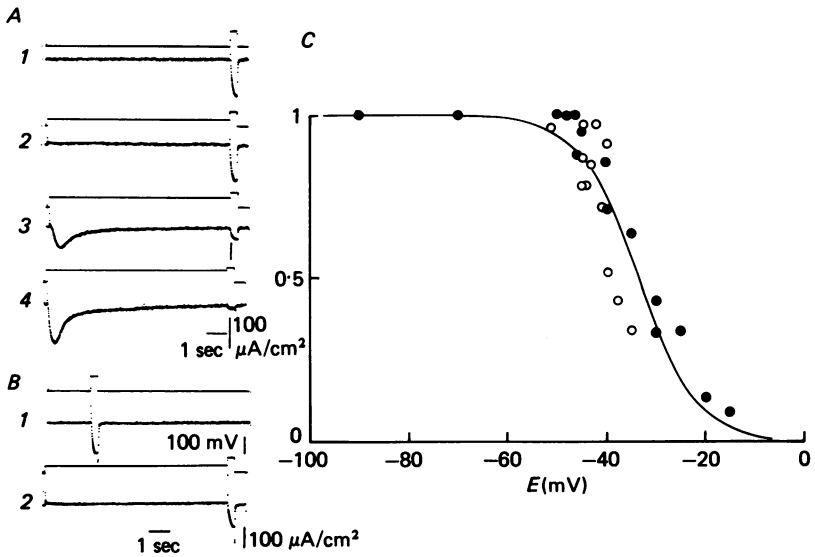

Fig. 6. Inactivation of Ca^{2+} currents. *A* and *B* from two different fibres. Same saline as in Fig. 1. Upper traces are voltages (pulse protocol) while lower ones are membrane currents. Membrane currents were not subtracted for linear components. Holding potential −90 mV. *C* shows the relation between I_{Ca} amplitude during the second pulse (to −10 mV) *vs.* the membrane potential during the first pulse in two different muscle fibres (normalized values). Smooth curve was drawn according to eqn. (3) (see text).

Results from two muscle fibres are plotted in Fig. 6*C*. At the holding potential of −90 mV Ca^{2+} channels were less than 3 % inactivated. The smooth curve was drawn according to the equation:

$$h_\infty = [1+\exp((E-E_{h\frac{1}{2}})/k_h)]^{-1} \quad (3)$$

where E is the prepulse potential, $E_{h\frac{1}{2}}$ the mid-point potential and k_h is a measure of the steepness of the curve. $E_{h\frac{1}{2}} = -33{\cdot}0$ mV and $k_h = 6{\cdot}3$ mV. Assuming that the decline of I_{Ca} during maintained depolarizations was entirely due to inactivation, we proceeded to determine the voltage dependence of τ_h, the time constant of inactivation, by fitting eqn. (2) with $a = 3$ (see below) to 20 % of the points of 1·8 sec digitized voltage-clamped currents. Only currents elicited by pulses to membrane potentials between −30 and +20 mV were used. Larger pulses were complicated by outward K^+ currents and smaller pulses by clamp inhomogeneity, since they were in the region of maximum $\partial G_{Ca}/\partial E$, thus producing notches in the current records.

The exponent of inactivation in eqn, (2) is 1 since I_{Ca} decayed following a single exponential. h_∞ was obtained from the steady-state inactivation curve (3) for membrane potentials more negative than -10 mV and was assumed to be zero for larger depolarizations. α_h and β_h were then calculated according to the equations:

$$\alpha_h = h_\infty/\tau_h, \tag{4}$$

$$\beta_h = (1-h_\infty)/\tau_h. \tag{5}$$

α_h and β_h were fitted to the functions proposed by Hodgkin & Huxley (1952)

$$\alpha_h = \bar{\alpha}_h \exp((E_h - E)/V_{\alpha h}), \tag{6}$$

$$\beta_h = \bar{\beta}_h/(1+\exp((E_h - E)/V_{\beta h})). \tag{7}$$

Open symbols in Fig. 8*B* are values of τ_h fitted to the experimental points with eqn. (2) and the smooth curve is the calculated τ_h from eqs. (6) and (7) with the parameters from Table 2. The low value of τ_h for -20 and -25 mV could be explained by clamp inhomogeneity in that region.

Activation of Ca^{2+} channels

The exponent of activation a was determined by fitting eqn. (2) to I_{Ca} with integer values of a between 1 and 4. Fig. 7 shows records of I_{Ca} (after subtraction of linear components) for a pulse to 0 mV, and the corresponding fitted curves. In each Figure, e is the experimental I_{Ca} and the numbers are the values of a for the fitted curves. It is clearly seen that the best fit was obtained for $a = 3$ (see Fig. 7*A* and *B*); records in *C* and *D* show another example at different sweep speeds with $a = 3$.

This procedure was carried out for membrane potentials between -30 mV and $+20$ mV and in general the fits were very good with $a = 3$. The standard deviation of the points from the fitted curve was less than 8 % of the peak amplitude. However the value $a = 3$ might be over-estimated because of clamp non-uniformities in the tubular system. For more negative potentials (-70 and 90 mV), τ_m was calculated from the relaxation time constant of tail currents multiplied by 3.

To calculate the rate constants of activation, α_m and β_m, the steady-state parameter of activation (m_∞) has to be determined. m_∞ can be obtained from A in eqn. (2) provided the current–voltage relation of open Ca^{2+} channels is known. Following the practice introduced by several authors for Na^+ channels (see for example Campbell & Hille, 1976) or other Ca^{2+} channels (for example, Reuter & Scholz, 1977), we assumed that the Goldman–Katz equation also applies to the Ca^{2+} channels of skeletal muscle:

$$I_{Ca} = \frac{4F^2EP_{Ca}}{RT}\frac{[Ca^{2+}]_o(\exp(2F(E-E_{Ca})/RT)-1)}{\exp(2FE/RT)-1}, \tag{8}$$

where F, R and T have the usual thermodynamic meanings, $E_{Ca} = +150$ mV (see Discussion) and P_{Ca} is the Ca^{2+} permeability. To account for the voltage dependence of Ca^{2+} activation, P_{Ca} can be expressed as:

$$P_{Ca} = \bar{P}_{Ca}\, m_\infty^3, \tag{9}$$

where $\bar{P}_{Ca}$ is the limiting Ca^{2+} permeability. Under the assumptions of eqn. (2), the amplitude factor A is determined by:

$$A = \frac{\bar{P}_{Ca} m_\infty^3 4F^2E[Ca^{2+}]_o (\exp(2F(E-E_{Ca})/RT)-1)}{RT\exp(2FE/RT)-1}. \quad (10)$$

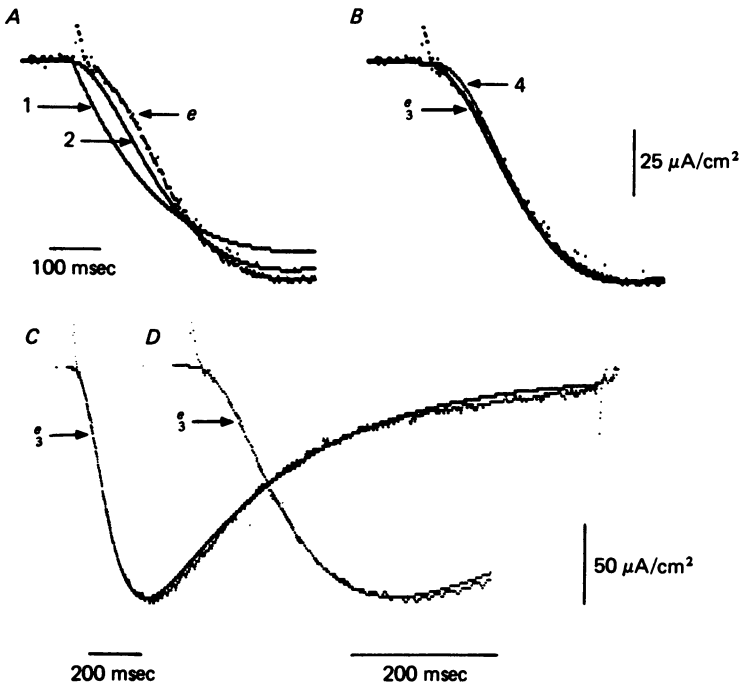

Fig. 7. Superimposed traces if I_{Ca} (e) and fitted curves were determined according to eqn (2). Pulse to 0 mV. Same saline as in Fig. 1. Membrane currents subtracted for linear components. A and B from the same fibre. Numbers close to the arrows correspond to values of a. C and D are the same record at two different sweep speeds. The noisier traces are I_{Ca} records.

The product $\bar{P}_{Ca} m_\infty^3$ was calculated according to eqn. (10) and its cube root was fitted to a function of the same form as eqn. (3)

$$(\bar{P}_{Ca} m_\infty^3)^{\frac{1}{3}} = \bar{P}_{Ca}[1+\exp((E_{m\frac{1}{3}}-E)/k_m)]^{-1}, \quad (11)$$

where $E_{m\frac{1}{3}}$ is the mid point, E is the test-pulse potential and k_m is a measure of the steepness. The fitting provided values of $\bar{P}_{Ca}$, $E_{m\frac{1}{3}}$ and k_m. The calculated values of the left-hand side of eqn. (11) were then normalized, averaged and fitted again to eqn. (11) to obtain the m_∞ curve shown in Fig. 8A. The symbols are averages of experimental points in different fibres and the curve is the m_∞ fitted function with $k_m = 9{\cdot}9$ mV and $E_{m\frac{1}{3}} = -35{\cdot}2$ mV. The average value of $\bar{P}_{Ca}$ is $1{\cdot}4 \pm 0{\cdot}4 \times 10^{-4}$ cm

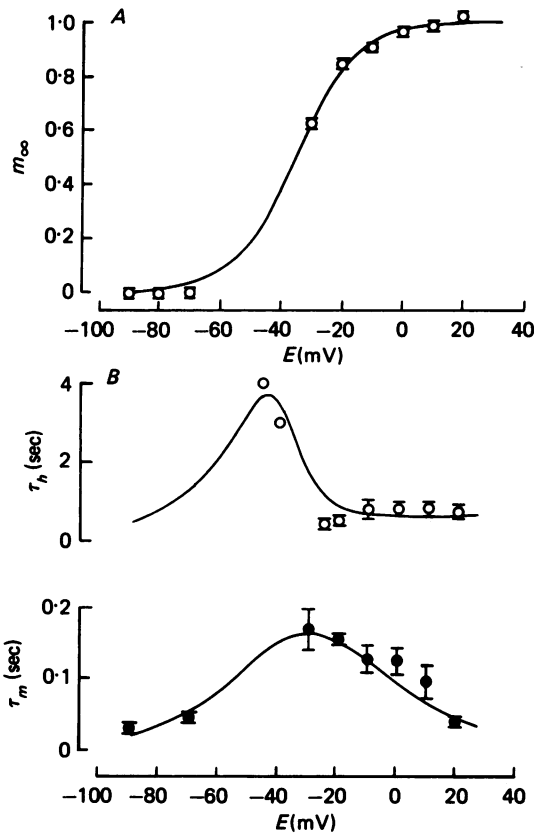

Fig. 8. *A*: m_∞ curve calculated as shown in the text. Points are mean values from two to five determinations; vertical bars are S.E. of means. Note that at 0 mV almost all the channels are activated. *B*, τ_h (upper curve) and τ_m (lower curve) as function of membrane potential (E). Points with bars are mean values from two to seven determinations; those without bars are single determinations. The curves were calculated according to eqns (6) and (7) (τ_h) and (12) and (13) (τ_m) with the parameters of Table 2.

sec^{-1} (5). α_m and β_m were calculated according to equations similar to (4) and (5) and fitted to the empirical functions:

$$\alpha_m = \frac{\bar{\alpha}_m(E-E_m)}{1-\exp\left((E_m-E)/V\alpha_m\right)}, \tag{12}$$

$$\beta_m = \bar{\beta}_m \exp\left((E_m-E)/V_{\beta m}\right). \tag{13}$$

The filled symbols in Fig. 8 *B* are averages of experimental values of τ_m and the smooth curve was drawn according to eqns, (10) and (11) with the parameters from Table 2. τ_m reaches a maximum of *ca.* 180 msec in −30 mV.

DISCUSSION

Comparison with previous work

This paper confirms and extends much of the previous work performed over the last few years on the Ca^{2+} current of skeletal muscle fibres of the frog (Stanfield, 1977; Sanchez & Stefani, 1978; Almers & Palade, 1981; Almers *et al.* 1981).

One of the major difficulties in the analysis of the Ca^{2+} current in the past has been the separation of other ionic currents, especially through K^+ channels. TEA is not completely effective in suppressing the delayed rectification of muscle and it is very ineffective in blocking the slow K^+ channels (Stanfield, 1970). Thus, even in isotonic

TABLE 2. Kinetic parameters of I_{Ca} following Hodgkin & Huxley model. For comparison the rate constants of Na channels are shown (Adrian *et al.* 1970). The values were corrected for 23 °C with a Q_{10} of 3·6 (Campbell & Hille, 1976)

	Activation			Inactivation	
	Ca^{2+}	Na^+		Ca^{2+}	Na^+
$\bar{\alpha}_m$	1·74 mV^{-1} sec^{-1}	0·52 mV^{-1} $msec^{-1}$	$\bar{\alpha}_h$	0·08 sec^{-1}	0·039 $msec^{-1}$
$\bar{\beta}_m$	0·12 sec^{-1}	5·3 $msec^{-1}$	$\bar{\beta}_h$	1·4 sec^{-1}	8·45 $msec^{-1}$
$\bar{E}_m$	−43·0 mV	—	$\bar{E}_h$	−25·5 mV	—
$V_{\alpha m}$	19·2 mV	—	$V_{\alpha h}$	19·7 mV	—
$V_{\beta m}$	23·1 mV	—	$V_{\beta h}$	6·1 mV	—
$\bar{P}_{Ca}$	$1{\cdot}4 \pm 0{\cdot}4 \times 10^{-4}$ cm sec^{-1} (5)			—	—

TEA, some K^+ currents persist unblocked (Sanchez & Stefani, 1978). For this reason we used, in addition to TEA, 3,4-DAP, a potent blocker of K^+ channels in the squid axon (Kirsch & Narahashi, 1978). In the reported experiments, 5 mM-3,4-DAP further blocked the remaining K^+ currents and improved the separation of Ca^{2+} currents up to +20 mV.

The Ca^{2+} current declined during a maintained depolarization and this decline was not due to residual K^+ contamination. This conclusion was supported by the following observations: (*a*) after abolishing the Ca^{2+} current by a Ca^{2+}-free Co^{2+} saline, K^+ currents were small and essentially stationary, (*b*) tail-current amplitudes to E_K measured at different times had a time course of decay similar to that of I_{Ca} decay (see also Adams & Gage, 1979). None the less, even with these two drugs in combination, K^+ blockage was inadequate for larger depolarizations. A better separation of the Ca^{2+} current has been achieved with the vaseline-gap technique where cut fibres are used and the removal of internal K^+ is possible (Almers & Palade, 1981).

Almers *et al.* (1981) have concluded, in view of extensive experimental evidence, that the decline of I_{Ca} can be explained by depletion of Ca^{2+} in the tubular system where most of the channels are located (Nicola Siri *et al.* 1980). Under their experimental conditions, the rate of decline was proportional to the amplitude of I_{Ca}, no matter how this amplitude was varied, either by drugs or by using cations with different permeabilities. Our work did not focus on the problem of depletion. Nevertheless, several observations do not agree with that interpretation for the intact fibre. The rate of decline did not greatly depend on I_{Ca} amplitude when D-600 was

used to block the channels. In fact, it was fairly constant for I_{Ca} not greater than 40 mA/cm^3 (Fig. 5). Furthermore, in our case we recorded I_{Ca} of about 40 mA/cm^3 which decayed with a time constant of 1 sec. Almers *et al.* (1981) recorded smaller currents which decayed much faster. For example I_{Ca} of about 35 mA/cm^3 decayed with a time constant of about 90 msec (Fig. 5 of Almers *et al.* 1981). Another discrepancy is the reduction of I_{Ca} by a prepulse which by itself failed to elicit a detectable I_{Ca} (Fig. 6). This observation was recently confirmed and extended by Cota, Nicola Siri & Stefani (1981*a*). On the other hand, Almers *et al.* (1981) reported that a conditioning prepulse reduced the amplitude of the test I_{Ca} only if it also activated I_{Ca}. To account for the observed 30% reduction of the test I_{Ca}, we calculated, assuming a linear activation of the Ca^{2+} current, a lower limit of 7 μA/cm^2 for the hypothetical peak I_{Ca} during the prepulse. Such amplitude is within the resolution of our techniques. Finally, as shown in Fig. 8*B*, τ_h did not change significantly between -10 mV and $+20$ mV, even though the amplitude of I_{Ca} changed as much as 50% in this range (Fig. 1*B*). In addition τ_h has been found to be very dependent on temperature ($Q_{10} = 3{\cdot}0$) and to be independent of I_{Ca} amplitude in inactivated Ca^{2+} currents (Cota, Nicola Siri & Stefani, 1981*a*, *b*).

The reasons for these discrepancies are not clear at present. Experimental conditions such as frog species, temperature, pH and ionic composition of external solutions, etc. were all the same. The major difference is that in our case we used intact fibres and block contraction with hypertonic sucrose, whereas in the other cases cut fibres were used and contraction was blocked with isotonic EGTA in the internal solutions. Hypertonic sucrose is known to produce swelling of the tubular system, leading to an increase in the tubular volume fraction (p) (Freygang, Goldstein, Hellam & Peachey, 1964) which would tend to cause less depletion.

Unfortunately E_{Ca}, which might provide a direct indication of tubular $[Ca^{2+}]_o$ is not measurable with the present techniques. Stanfield (1977) reported, in *Rana temporaria*, an apparent reversal potential for I_{Ca} of *ca.* +18 mV. In our experiments, with a better blockage of K^+ channels, we found a reversal potential of *ca.* +40 mV, and Almers & Palade (1981) still recorded inward I_{Ca} at +50 mV. E_{Ca} should be far more positive than those estimates. In addition, as pointed out by Hagiwara & Byerly (1981), the extrapolation of I–V curves is an unreliable method for estimating E_{Ca}. For our calculations we assumed a conservative E_{Ca} of +150 mV.

Kinetic properties

Evidence has accumulated that the Ca^{2+} channels are located in the membranes of tubular system (Nicola Siri *et al.* 1980; Almers *et al.* 1981) where direct access to electrical recording is not possible. This is of course, a major problem in the kinetic analysis of the channels. In our experiments all other tubular ionic channels were blocked, and since I_{Ca} is very slow it is likely that the tubular system was better controlled than in other voltage-clamp experiments, but it is not straightforward to have a quantitative estimate of the tubular potential when the surface membrane is clamped. Hille & Campbell (1976) reported that, because of the luminal resistance, only 21% of active tubular Na^+ channels were seen at the surface, producing notches in their current traces which were significant for small depolarizations. We also observed in our experiments notches in $V_2 - V_1$ traces for membrane potentials more

negative than −30 mV but they were not apparent for larger depolarizations. Adrian & Peachey (1973) also calculated tubular currents and axial potentials during a voltage clamp in a region close to 0 mV and concluded that surface and tubular potentials may differ substantially.

In both examples, the kinetic properties of the tubular channels were assumed to be identical to those of the surface channels. We cannot make similar assumptions for the Ca^{2+} channels since they were not measurable at the surface and Ca^{2+} channels differ widely in their kinetics from one preparation to another. For example, Adams & Gage (1979) reported values of τ_h ranging from *ca.* 50 to *ca.* 275 msec for Ca^{2+} channels of *Aplysia* neurones, whereas τ_h of Ca^{2+} channels of skeletal muscle ranges from *ca.* 1 to *ca.* 4 sec (Fig. 8*B*); furthermore inactivation was negligible in the presynaptic terminal in the squid giant synapse (Llinás, Steinberg & Walton, 1981). In spite of these difficulties, the kinetic model seems to be a fair description of the experimental data (Fig. 7) and the voltage dependences of τ_m and τ_h are satisfactorily described.

If the parameters from Table 2 describe adequately the kinetic properties of the Ca^{2+} channels of skeletal muscle, one may calculate the influx of Ca^{2+} during a single action potential and compare it with data obtained with different techniques. This should provide a first approximation in testing the accuracy of the model. As a first attempt we considered a simple RC circuit, and used the rate constants of Campbell & Hille (1976) for Na^+ channels and those of Adrian *et al.* (1970) for K^+ channels, corrected to room temperature by a Q_{10} of 3·6, and incorporated the parameters of our model and the mean G_m and C_m of our fibres. The Ca^{2+} channels are roughly one thousand times slower than Na^+ channels and have about one tenth of their maximum permeability (Campbell & Hille, 1976). We obtained an influx of 0·06 p-mole/cm^2 of external surface per action potential. Curtis (1966) measured 1 p-mole/cm^2 per twitch and recently Bianchi & Narayan (1982) measured 1·3 p-mole/cm^2 per twitch. Our results are about one order of magnitude smaller and agree with the calculations of Almers & Palade (1981) based on the estimation of the area under I_{Ca} during tail current. The difference between the tracer data and our calculations might be due to the many assumptions and approximations of our model but could also be done to the very different experimental conditions between the tracer experiments and our ours.

The authors are indebted to Arturo Aldana for his assistance with the computer programming, to David Elias for building electronic equipment, to Leonardo Nicola Siri for helpful discussions during the experiments and to Emma Bensimón for her secretarial work. We are grateful to Dr Wolfhard Almers for reading the manuscript. This work was supported by the CONACyT of México, Grant PCCBNAL 790022.

REFERENCES

ADAMS, D. J. & GAGE, P. W. (1979). Characteristics of sodium and calcium conductance changes produced by membrane depolarization in an *Aplysia* neurone. *J. Physiol.* **289**, 143–161.

ADRIAN, R. H., CHANDLER, W. K. & HODGKIN, A. L. (1970). Voltage clamp experiments in striated muscle fibres. *J. Physiol.* **208**, 607–644.

ADRIAN, R. H. & PEACHEY, L. D. (1973). Reconstruction of the action potential of frog sartorius muscle. *J. Physiol.* **235**, 103–131.

ALMERS, W., FINK, R. & PALADE, P. T. (1981). Calcium depletion in frog muscle tubules: the decline of calcium current under maintained depolarization. *J. Physiol.* **312**, 177–207.

ALMERS, W. & PALADE, P. T. (1981). Slow calcium and potassium currents across frog muscle membrane: measurements with a vaseline-gap technique. *J. Physiol.* **312**, 159–176.

BEATY, G. N. & STEFANI, E. (1976*a*). Calcium dependent electrical activity in twitch muscle fibres of the frog. *Proc. R. Soc.* B **194**, 141–150.

BEATY, G. N. & STEFANI, E. (1976*b*). Inward calcium current in twitch muscle fibres of the frog. *J. Physiol.* **260**, 27*P*.

BIANCHI, C. P. & NARAYAN, S. (1982). Muscle fatigue and the role of transverse tubules. *Science, N.Y.* **215**, 295–296.

CAMPBELL, D. T. & HILLE, R. (1976). Kinetic and pharmacological properties of the sodium channel of frog skeletal muscle. *J. gen. Physiol.* **67**, 309–323.

CHANDLER, W. K., RAKOWSKI, R. F. & SCHNEIDER, M. F. (1976). A non-linear voltage dependent charge movement in frog skeletal muscle. *J. Physiol.* **254**, 245–283.

COLQUHOUN, D. (1971). *Lectures on Biostatistics.* Oxford: Clarendon Press.

COTA, G., NICOLA SIRI, L. & STEFANI, E. (1981*a*). Calcium current decay in frog skeletal muscle fibres: inactivation and/or depletion from TTS. *Proc. VII International Biophysics Congress*, p. 227.

COTA, G., NICOLA SIRI, L. & STEFANI, E. (1981*b*). Ca current in frog skeletal muscle fibres: effect of temperature on I_{Ca} decay. In *The Mechanism of Gated Calcium Transport across Biological Membranes*, ed. OHNISHI, S. TSUYOSHI & ENDO MAKOTO. New York: Academic Press.

CURTIS, B. A. (1966). Ca fluxes in single twitch muscle fibers. *J. gen. Physiol.* **50**, 255–267.

FINK, R. & LÜTTGAU, H. C. (1976). An evaluation of the membrane constants and the potassium conductance in metabolically exhausted muscle fibres. *J. Physiol.* **263**, 215–238.

FREYGANG, W. H., JR., GOLDSTEIN, D. A., HELLAM, D. C. & PEACHEY, L. D. (1964). The relation between the late after-potential and the size of the transverse tubular system of frog muscle. *J. gen. Physiol.* **48**, 235–263.

HAGIWARA, S. & BYERLY, L. (1981). Calcium channel. *Rev. Neurosci.* **4**, 69–125.

HILLE, B. & CAMPBELL, D. T. (1976). An improved vaseline gap voltage clamp for skeletal muscle fibers. *J. gen. Physiol.* **67**, 265–293.

HODGKIN, A. L. & HUXLEY, A. F. (1952). A quantitative description of membrane current and its application to conduction and excitation in nerve. *J. Physiol.* **117**, 500–544.

KIRSCH, G. E. & NARAHASHI, T. (1978). 3,4-diaminopyridine: a potent new potassium channel blocker. *Biophys. J.* **22**, 507–512.

LLINÁS, R., STEINBERG, I. Z. & WALTON, K. (1981). Presynaptic calcium currents in squid giant synapse. *Biophys. J.* **33**, 289–322.

MCDONALD, T. F., PELZER, D. & TRAUTWEIN, W. (1980). On the mechanism of slow calcium channel block in heart. *Pflügers Arch.* **385**, 175–179.

NICOLA SIRI, L., SÁNCHEZ, J. A. & STEFANI, E. (1980). Effect of glycerol treatment on the calcium current of frog skeletal muscle. *J. Physiol.* **305**, 87–96.

PALLOTA, S. B., MAGLEBY, K. L. & BARRETT, J. N. (1981). Single channel recordings of Ca^{2+}-activated K currents in rat muscle cell culture. *Nature, Lond.* **293**, 471–474.

REUTER, H. & SCHOLZ, H. (1977). A study of the ion selectivity and the kinetic properties of the calcium dependent slow inward current in mammalian cardiac muscle. *J. Physiol.* **264**, 17–47.

SÁNCHEZ, J. A. & STEFANI, E. (1978). Inward calcium current in twitch muscle fibres of the frog. *J. Physiol.* **283**, 197–209.

SÁNCHEZ, J. A. & STEFANI, E. (1980). Kinetics of Ca^{2+} current in frog skeletal muscle. *Fedn Proc.* **39**, 2075.

SCHNEIDER, M. F. & CHANDLER, W. K. (1973). Voltage dependent charge movement in skeletal muscle: a possible step in excitation contraction coupling. *Nature, Lond.* **242**, 244–246.

STANFIELD, P. R. (1970). The effect of the tetraethylammonium ion on the delayed currents of frog skeletal muscle. *J. Physiol.* **209**, 209–229.

STANFIELD, P. R. (1977). A calcium dependent inward current in frog skeletal muscle fibres. *Pflügers Arch.* **368**, 267–270.

STEFANI, E., SÁNCHEZ, J. A. & NICOLA SIRI, L. (1981). Calcium currents in twitch muscle fibres of the frog. In *Adv. Physiol. Sci. Vol. 5. Molecular and Cellular aspects of muscle function*, ed. VARGA, E., KOVÉR, A., KOVÁCS, T. & KOVACS, L. Budapest: Pergamon Press.